In vivo measurements of the triceps surae complex architecture in man: implications for muscle function

Constantinos N. Maganaris, Vasilios Baltzopoulos and Anthony J. Sargeant*

*Biomechanics and Neuromuscular Biology Research Groups, Manchester Metropolitan University, Alsager ST7 2HL, UK and *Institute for Fundamental and Clinical Human Movement Sciences, Faculty of Human Movement Sciences, Vrije Universiteit, 1081 BT Amsterdam, The Netherlands*

(Received 23 March 1998; accepted after revision 10 July 1998)

1. The objectives of this study were to (1) quantify experimentally *in vivo* changes in pennation angle, fibre length and muscle thickness in the triceps surae complex in man in response to changes in ankle position and isometric plantarflexion moment and (2) compare changes in the above muscle architectural characteristics occurring in the transition from rest to a given isometric plantarflexion intensity with the estimations of a planimetric muscle model assuming constant thickness and straight muscle fibres.

2. The gastrocnemius medialis (GM), gastrocnemius lateralis (GL) and soleus (SOL) muscles of six males were scanned with ultrasonography at different sites along and across the muscle belly at rest and during maximum voluntary contraction (MVC) trials at ankle angles of −15 deg (dorsiflexed direction), 0 deg (neutral position), +15 deg (plantarflexed direction) and +30 deg. Additional images were taken at 80, 60, 40 and 20 % of MVC at an ankle angle of 0 deg.

3. In all three muscles and all scanned sites, as ankle angle increased from −15 to +30 deg, pennation increased (by 6–12 deg, 39–67 %, $P < 0{\cdot}01$ at rest and 9–16 deg, 29–43 %, $P < 0{\cdot}01$ during MVC) and fibre length decreased (by 15–28 mm, 32–34 %, $P < 0{\cdot}01$ at rest and 8–10 mm, 27–30 %, $P < 0{\cdot}05$ during MVC). Thickness in GL and SOL increased during MVC compared with rest (by 5–7 mm, 36–47 %, $P < 0{\cdot}01$ in GL and 6–7 mm, 38–47 %, $P < 0{\cdot}01$ in SOL) while thickness of GM did not differ ($P > 0{\cdot}05$) between rest and MVC.

4. At any given ankle angle the model underestimated changes in GL and SOL occurring in the transition from rest to MVC in pennation angle (by 9–12 deg, 24–38 %, $P < 0{\cdot}01$ in GL and 9–14 deg, 25–28 %, $P < 0{\cdot}01$ in SOL) and fibre length (by 6–15 mm, 22–39 %, $P < 0{\cdot}01$ in GL and 6–8 mm, 23–24 %, $P < 0{\cdot}01$ in SOL).

5. The findings of the study indicate that the mechanical output of muscle as estimated by the model used may be unrealistic due to errors in estimating the changes in muscle architecture during contraction compared with rest.

The obliqueness of the fibres of a muscle in relation to the force-generating axis of the muscle–tendon complex is known as the pennation angle and its magnitude is an important determinant of the muscle's functional characteristics (Gans & Bock, 1965; Gans, 1982; Otten, 1988; Fukunaga *et al.* 1997). For a given muscle anatomical cross-sectional area and volume, an increased pennation angle results in a reduced muscle fibre length, compromising shortening velocity and excursion range, but also allows more contractile material to be placed in parallel, increasing maximum force generation (Alexander & Vernon, 1975; Gans, 1982; Muhl, 1982). Therefore, the maximum force produced at a given muscle fibre length in the direction of the fibres in a pennate muscle is higher than the maximum force produced in the direction of the fibres of a parallel-fibre muscle of the same anatomical cross-sectional area and volume. However, pennation angle itself also results in a tendon force loss proportional to 1 − cosine of the pennation angle. Thus, an increasing pennation angle only up to 45 deg could theoretically result in an increase both in force produced in the direction of muscle fibres and in its effective component transmitted to the tendon (Alexander & Vernon, 1975; Rutherford & Jones, 1992).

Accurate information with respect to pennation angle is important in two types of analysis: first, when the joint moment that a muscle can exert is calculated from the force

that a muscle is predicted to produce in the direction of its fibres (e.g. Woittiez *et al.* 1983; Zajac, 1989), and secondly and inversely, when force production in the direction of a muscle's fibres is calculated from the moment-generating capacity of the muscle (e.g. Narici *et al.* 1992; Kawakami *et al.* 1994). The pennation angle of a muscle can be, and often has been, obtained by direct anatomical inspections on cadaveric specimens (Alexander & Vernon, 1975; Wickiewicz *et al.* 1983; Woittiez *et al.* 1983; Frendrich & Brand, 1990; Spoor *et al.* 1991). However, values taken from embalmed muscles do not represent *in vivo* dimensions (Yamaguchi *et al.* 1990) and are unlikely to reflect accurately architectural changes experimentally observed under *in vivo* or *in situ* conditions. Furthermore, pennation angle changes inversely as a function of muscle fibre length (Muhl, 1982; Huijing & Woittiez, 1984; Ichinose *et al.* 1995; Narici *et al.* 1996), and proportionally as a function of isometric force generated by the muscle (Herbert & Gandevia, 1995; Ichinose *et al.* 1995; Narici *et al.* 1996) so that the muscle's fibre volume is kept constant at different lengths and contracted stages (Baskin & Paolini, 1967). Differences have been reported for human muscle pennation angle values of up to 120–170% between rest and maximum isometric contractions at a given joint angle (Herbert & Gandevia, 1995; Narici *et al.* 1996). Clearly, failure to consider this contraction effect on pennation angle may be a source of serious error in any calculations of muscle force and joint moment.

Several theoretical models estimate changes in the pennation angle of a muscle as a function of fibre length alteration, making the assumption that muscle thickness (distance between aponeuroses) remains constant as the fibres shorten or lengthen (Huijing & Woittiez, 1984; Woittiez *et al.* 1984; Zajac, 1989; Spoor *et al.* 1991). However, it has been shown that muscle thickness may change during contraction (Zuurbier & Huijing, 1993; Herbert & Gandevia, 1995; Ichinose *et al.* 1995) and the validity of results derived from analyses assuming constant thickness may thus be questionable.

In an attempt to improve our understanding of *in vivo* changes of muscle architecture, modern imaging techniques have been used (Henriksson-Larsen *et al.* 1992; Narici *et al.* 1992, 1996, 1998; Kawakami *et al.* 1993; Herbert & Gandevia, 1995; Ichinose *et al.* 1995; Fukunaga *et al.* 1997). Real-time ultrasonography enables *in vivo* muscle scanning and offers promise for a realistic determination of changes in muscle architecture (Rutherford & Jones, 1992; Kawakami *et al.* 1993; Narici *et al.* 1996). Real-time ultrasonic measurements were taken in the present study in the triceps surae muscle in man. The purpose of our research work was to (1) determine *in vivo* changes in pennation angle and fibre length in each muscle of the triceps surae complex (gastrocnemius medialis (GM), gastrocnemius lateralis (GL) and soleus (SOL)) as a function of ankle joint angle and moment produced voluntarily during an isometric ankle plantarflexion and (2) evaluate the accuracy of estimating changes in muscle architecture in the transition from rest to a given isometric plantarflexion moment using a planimetric model assuming constant thickness and straight fibres (Huijing & Woittiez, 1984). Morphometric analysis of *in vivo* muscle scans would enhance our understanding of the mechanical behaviour of living muscles and enable evaluation of the applicability of simple planimetric models in estimating loads in the musculoskeletal system.

METHODS

Subjects

Six healthy males, from whom written informed consent had previously been obtained, volunteered to participate in this study. All subjects were physically active, but no one had previously taken part in regular weight training. None had any subjective clinical evidence of musculoskeletal injury or any orthopaedic abnormality. Their mean (± S.D.) age, height and body mass were 28 ± 3 years, 175 ± 8 cm and 75 ± 5 kg, respectively. The study was approved by the Manchester Metropolitan University ethics committee.

Plantarflexion moment measurements

Seven days prior to the experimental trial (data collection), a familiarization trial was undertaken to acquaint the subjects with the test requirements and determine their stronger leg. Subjects performed a series of isometric plantarflexion contractions on an isokinetic dynamometer (Lido Active, Loredan Biomedical, Davis, CA, USA) at ankle angles of −15 deg (dorsiflexed direction), 0 deg (neutral ankle position: the footplate of the dynamometer perpendicular to the longitudinal axis of the tibia), +15 deg (plantarflexed direction) and +30 deg. All measurements were carried out with the knee joint flexed at 90 deg. Both the foot and the knee of the tested leg were securely fixed at the required position by means of Velcro straps and mechanical stops which prevented any observable heel lift during maximal plantarflexion. Nevertheless, it is recognized that there is a degree of compression of soft tissue in the plantar surface of the foot during such contractions and this will result in a slight movement of the joint with respect to the footplate introducing a small measurement error. The subjects were verbally encouraged to perform static contractions with the ankle plantarflexor with a maximum possible effort at all four ankle angles, and they were encouraged to hold each contraction for about 2–3 s. Contractions were performed in a randomized order. Three contractions were performed at each ankle angle by allowing a 1 min rest interval between bouts and the highest value was considered the maximum voluntary contraction (MVC; the maximum isometric voluntary plantarflexion moment) at that ankle angle. The stronger leg was defined as the one with the highest MVC. Each subject was then asked to maintain the stronger leg contractions for at least 2–3 s at 80, 60, 40 and 20% of MVC at the neutral ankle position (0 deg). Subjects were given visual feedback of the target and elicited force on a computer screen.

Ultrasound scanning

Ultrasound images were obtained during the experimental trial on the previously determined stronger leg. A real-time B-mode ultrasound apparatus (Esaote Biomedica AU3 Partner, Florence, Italy) with a 7·5 MHz linear-array probe was used to obtain sagittal images of the GM, GL and SOL at rest and at 100% of plantarflexor MVC at all four ankle angles, and at 80, 60, 40 and 20% of plantarflexor MVC at the neutral ankle position. The scanning head of the probe was coated with transmission gel to obtain acoustic coupling, and oriented along the mid-sagittal axis of each muscle. Sonographs were taken after having adjusted the

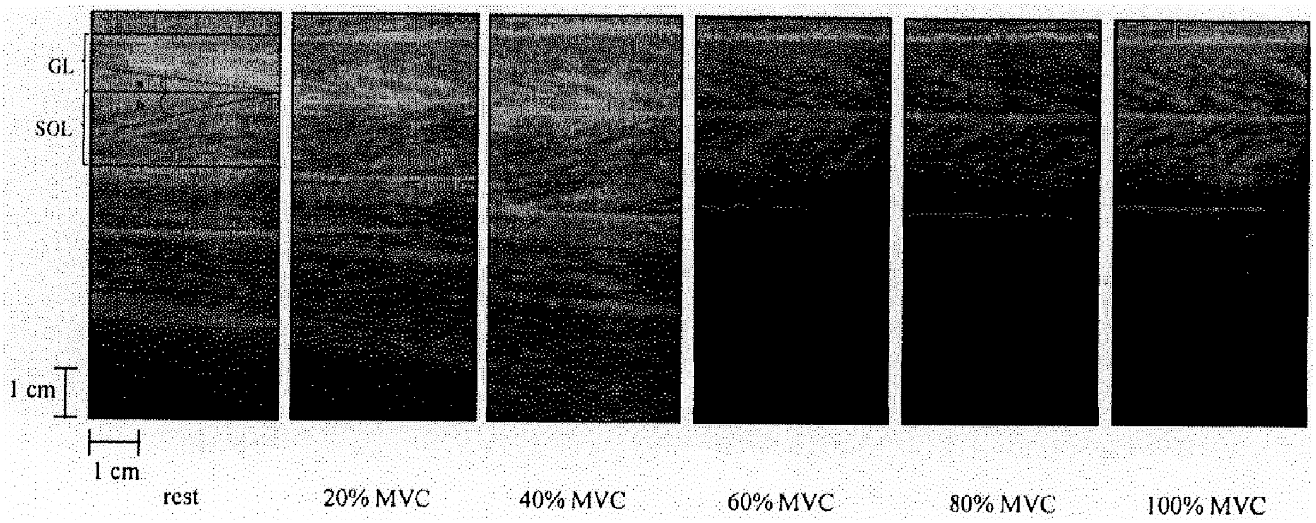

Figure 1. Sonographs of GL and SOL

Sagittal sonographs of GL and SOL at the neutral ankle position at rest, 20, 40, 60, 80 and 100% of an ankle plantarflexor MVC. The presented sonographs were taken with the scanning head of the probe positioned at the central region over the SOL mid-sagittal axis (region C and section MS in Fig. 3). The horizontal stripes are ultrasonic waves reflected from the superficial and deep aponeuroses of each muscle and the oblique stripes are echoes derived from fascia septas between muscle fascicles. The fascicles' length and angulation with respect to the aponeuroses were adopted to represent the muscle's fibre length and pennation angle, respectively. a, GL pennation angle; b, SOL pennation angle.

depth gain compensation to optimize image quality. At rest and during contractions, the probe was firmly held against the skin at the same site over the muscle belly. All images obtained were recorded on a videotape and then analysed. Acquired images during contraction were analysed at the time point at which each target plantarflexion moment reached its plateau value. Muscle thickness was measured as the distance between the superficial and the deep aponeurosis echoes, and fibre length (fascicle length) at rest was measured as the length of the line drawn along the echoes parallel to the fascicles from the deep up to the superficial aponeurosis (Ichinose *et al.* 1995; Narici *et al.* 1996; Fukunaga *et al.* 1997) (Fig. 1). Fascicle length during contraction was measured as the length of the straight line between the insertion points of the fascicle, onto the aponeurosis of the muscle. The angle between the fascicles echo and the aponeurosis echo was defined as the muscle's pennation angle (Rutherford & Jones, 1992; Kawakami *et al.* 1993; Narici *et al.* 1996; Fukunaga *et al.* 1997) (Fig. 1). In each muscle scan, the inter-aponeuroses area was divided into three horizontal bands by two parallel straight lines: line 1 towards the superficial aponeurosis and line 2 towards the deep aponeurosis (Fig. 2). For all three muscles the intersection point between line 1 and a fascicle was identified. The straight line (S_1) passing through the latter point and the insertion point of that fascicle onto the superficial aponeurosis of the muscle was drawn. The angle between that line

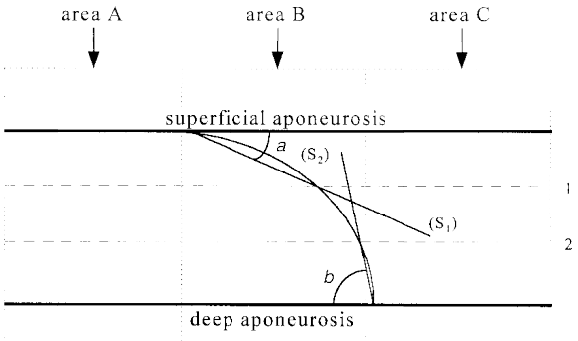

Figure 2. Pennation angle measurements

The diagram shown represents a sagittal muscle sonograph of gastrocnemii. The curved line between aponeuroses represents a fascicle. Lines 1 and 2 divide the area between aponeuroses into three horizontal bands of equal dimensions. Lines S_1 and S_2 pass through the intersection point between the fascicle and the lines 1 and 2, respectively, and the insertion point of the fascicle onto the superficial and deep aponeurosis of the muscle. *a* and *b* are digitized pennation angles on the superficial and deep aponeurosis, respectively. The vertical bands A, B and C represent the three different areas analysed to establish whether architecture was constant along the image.

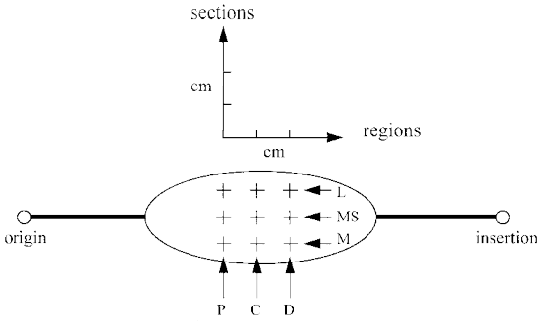

Figure 3. Representation of the different sites from which sagittal sonographs were taken

The posterior aspect of a muscle in the calf of the right leg is presented. P, C and D represent proximal, central and distal regions, respectively. L, MS and M represent lateral, mid-sagittal and medial sections, respectively.

and the superficial aponeurosis of the muscle (angle a in Fig. 2) was adopted to represent the muscle's pennation angle. Measurements of pennation angle and fibre length and thickness were derived from enlarged images using a computerized sonic digitizer (TDS, Blackburn, UK).

To establish whether the architectural profile was constant at rest throughout the belly of each muscle, a series of images were taken from all subjects at different sites at the neutral ankle position. Along the mid-sagittal axis of GM, GL and SOL, three regions about 2 cm apart, a proximal, a central and a distal one relative to each muscle origin, were imaged (Fig. 3). Additionally, images were taken in three subjects of sections about 2 cm lateral and 2 cm medial to a given probe placement at the mid-sagittal axis of the muscle (Fig. 3). All sites from which images were taken at rest were also imaged during MVC in order to establish whether muscle architecture remained constant along and across the muscle's belly during contraction. On each image and muscle, three areas, that is both sides and the middle area (areas A, B and C in Fig. 2), were analysed to establish whether architectural characteristics were constant along the images.

Muscle modelling

GM, GL and SOL, both at rest and at all contraction intensities and ankle positions, were modelled as two-dimensional parallelograms (Huijing & Woittiez, 1984) (Fig. 4). The major geometrical assumptions made when using such planimetric models are that (1) aponeuroses behave as rigid bodies and run parallel to each other and (2) muscle fibres run straight between aponeuroses. As a result of the above assumptions, inter-aponeuroses distance (muscle thickness) remains constant in response to changes in muscle length. For a constant thickness in the transition from an initial to a final muscle length, $\sin a \times Lf_1 = \sin b \times Lf_2$, where a and b are initial and final pennation angles, respectively, and Lf_1 and Lf_2 are initial and final fibre lengths, respectively. This is the equation used in the present study to obtain estimated values of pennation angle and fibre length during a given state of contraction at a given ankle angle. Actual pennation angle and fibre length measurements at rest and actual measurements of fibre length at a given state of contraction were used as input to the above equation to derive estimated pennation angle values during contraction. For calculations of the estimated fibre length at a given state of contraction, actual measurements of pennation angle at rest and during contraction and actual resting fibre length measurements were used as input to the equation. Measurements from the central region along the mid-sagittal axis of each muscle were incorporated in the equation.

Statistical treatment

Descriptive statistics calculations included means and standard deviations. Differences in pennation angles, fibre lengths and thicknesses between rest and MVC and between different ankle angles were tested using two-way analysis of variance tests. Two-way analysis of variance tests were also used to test differences between actual pennation angles and fibre lengths and those estimated by the model. Simple effects tests were used to identify where interaction effects occurred. Tukey's test was used to determine significant differences between mean values. One-way analysis of variance was used to determine differences in pennation angle, fibre length and thickness between (1) different areas of a given image (areas A, B and C in Fig. 2), (2) different regions over the mid-sagittal axis of the muscle belly (regions P, C and D over the section MS in Fig. 3) and (3) different contraction intensities at the neutral ankle position in each muscle in all six subjects. Friedman's rank test was used to test differences in pennation angle, fibre length and thickness between all nine different scanned sites (Fig. 3) over a given muscle in three of the subjects of the study. Regression models were used to determine the relationship between pennation angle and plantarflexion moment (%MVC) in all three muscles. A level of $P < 0{\cdot}05$ was selected to indicate statistical significance.

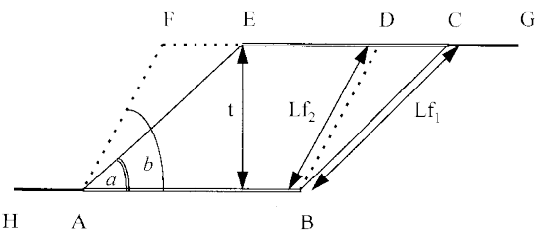

Figure 4. Representation of the planimetric muscle model used in the study

ABCE, muscle at rest; ABDF, muscle at the contracted state. a and b, pennation angles at rest and the contracted state, respectively. Lf_1 and Lf_2, fibre lengths at rest and the contracted state, respectively. t, muscle thickness, constant in the transition from rest to the contracted state.

RESULTS

Architectural profile along and across the muscle belly

For each individual muscle, in three of the six subjects, a total of eighteen images from different regions and sections were analysed for pennation angle, fibre length and thickness. Nine images were acquired at rest and nine images were acquired during MVC. In the three subjects, no significant difference was found at rest and during MVC in pennation angle, fibre length and thickness between different scanned regions and sections over a given muscle (Tables 1–3). In all six subjects, no significant difference was found when comparing pennation angle, fibre length and thickness of a given muscle, either at rest or during MVC, between (1) different areas of a given image and (2) different regions over the mid-sagittal axis of the muscle belly.

Architectural characteristics at rest

Thicknesses of GM, GL and SOL at rest (~17, 15 and 15 mm, respectively) did not change significantly in response to changes in muscle length resulting from changes in ankle joint angle (Fig. 5*A*). In all three muscles at rest, pennation angle and fibre length were ankle angle dependent. In all three muscles, as ankle angle increased from −15 deg to +30 deg, the pennation angle increased: in GM from $17{\cdot}8 \pm 2{\cdot}1$ to $25{\cdot}2 \pm 2{\cdot}0$ deg (39%, $P < 0{\cdot}01$), in GL from $9 \pm 1{\cdot}3$ to $15 \pm 2{\cdot}0$ deg (67%, $P < 0{\cdot}05$) and in SOL from $21{\cdot}3 \pm 3{\cdot}2$ to $33{\cdot}3 \pm 3{\cdot}3$ deg (57%, $P < 0{\cdot}01$). In all three muscles, as ankle angle increased from −15 deg to +30 deg, fibre length decreased: in GM from 53 ± 3 to $36 \pm 1{\cdot}5$ mm (32%, $P < 0{\cdot}01$), in GL from 83 to 55 mm (34%, $P < 0{\cdot}01$) and in SOL from $42{\cdot}5 \pm 3$ to $27{\cdot}6 \pm 3{\cdot}6$ mm (33%, $P < 0{\cdot}01$).

Architectural characteristics during MVC

Thicknesses of GM, GL and SOL during MVC (~17, 22 and 21 mm, respectively) did not change significantly in response to changes in muscle length ($P < 0{\cdot}05$ only in combinations of an ankle angle of +30 deg in GL) (Fig. 5*B*). In all three muscles during MVC, pennation angle and fibre length were ankle angle dependent. In all three muscles, as ankle angle increased from −15 to +30 deg, the pennation angle increased: in GM from $37 \pm 2{\cdot}3$ to $52{\cdot}9 \pm 2{\cdot}6$ deg (43%, $P < 0{\cdot}01$), in GL from $32 \pm 2{\cdot}9$ to $41{\cdot}3 \pm 2{\cdot}7$ deg (29%, $P <$

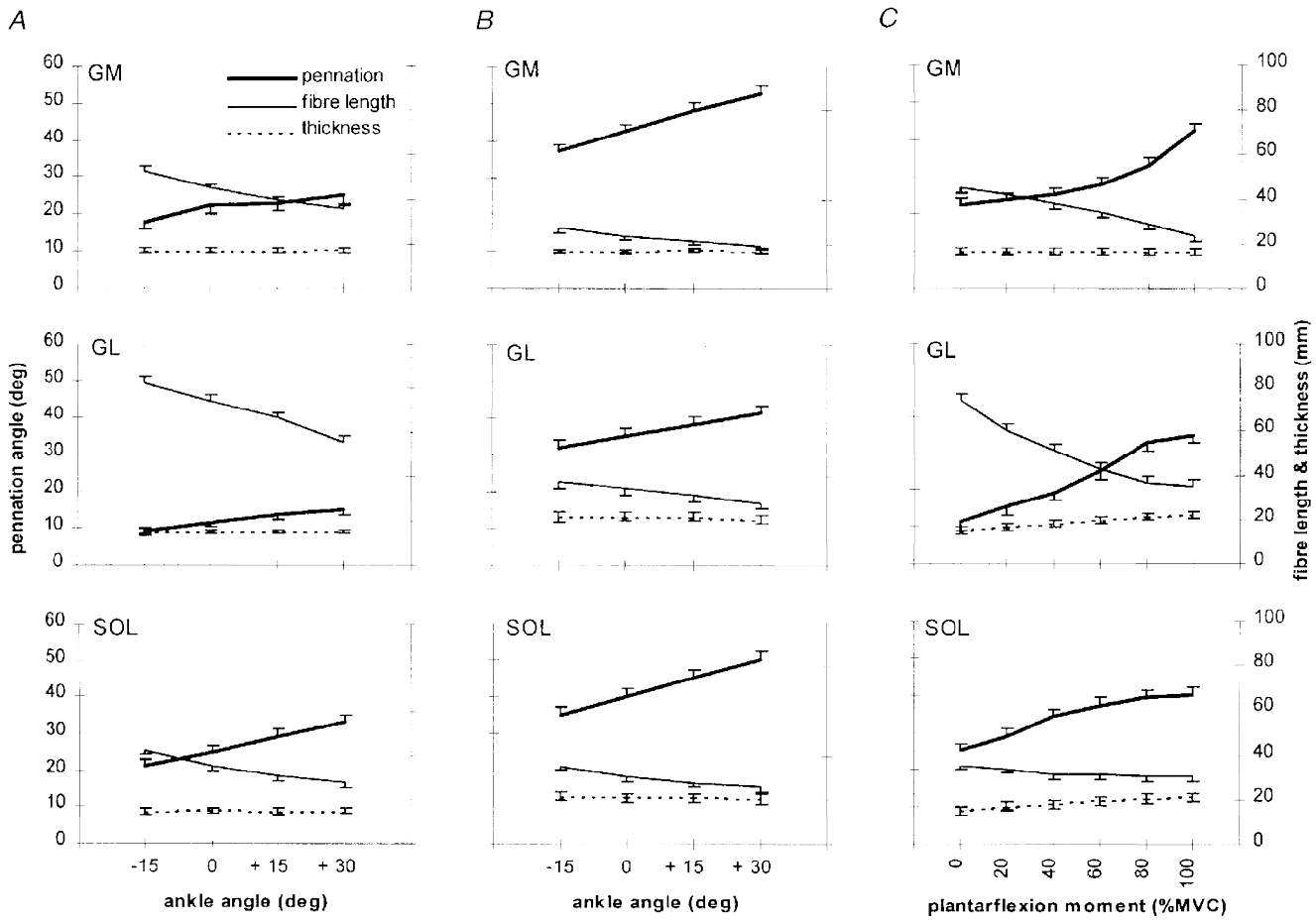

Figure 5. Changes in the triceps surae complex architecture

A, changes at rest as a function of ankle angle; *B*, changes during MVC as a function of ankle angle; *C*, changes during graded isometric plantarflexion at the neutral ankle position in GM, GL and SOL. Notice the increase in GL and SOL thickness as a function of plantarflexion moment. Values were derived from sonographs at the central region over the mid-sagittal axis of each muscle. Values are means ± S.D. ($n = 6$).

Table 1. GM architecture

	Pennation angle (deg)			Fibre length (mm)			Thickness (mm)		
	P	C	D	P	C	D	P	C	D
Rest									
M	21·4 ± 1·1	21·8 ± 1·4	21·5 ± 2·1	43·0 ± 2·0	43·9 ± 2·2	44·1 ± 1·7	16·3 ± 2·0	16·6 ± 1·0	17·0 ± 2·0
MS	21·5 ± 2·0	22·3 ± 2·0†	22·3 ± 1·7	45·9 ± 3·1	45·0 ± 2·3†	45·2 ± 2·2	17·6 ± 2·6	17·1 ± 1·3†	17·0 ± 1·6
L	22·0 ± 2·1	22·1 ± 1·9	22·3 ± 2·0	45·4 ± 2·3	45·0 ± 1·8	45·0 ± 3·0	17·6 ± 1·6	17·0 ± 1·4	17·3 ± 3·1
MVC									
M	42·5 ± 2·5	41·7 ± 1·9	41·5 ± 3·2	25·0 ± 1·5	23·0 ± 1·9	22·6 ± 2·2	16·8 ± 2·0	16·5 ± 1·0	17·2 ± 2·2
MS	43·4 ± 2·9	42·5 ± 2·2†	43·0 ± 3·4	25·0 ± 3·0	23·4 ± 1·9†	24·4 ± 1·9	17·0 ± 2·5	16·9 ± 1·5†	17·0 ± 2·0
L	42·0 ± 3·4	42·4 ± 2·2	42·6 ± 2·0	23·0 ± 2·0	23·0 ± 2·2	24·0 ± 2·0	17·1 ± 2·0	16·8 ± 1·2	16·5 ± 2·9

Analysis of GM architecture at the neutral ankle position along (regions P, C and D) and across (sections M, MS and L) its belly (see Fig. 3), at rest and during an ankle plantarflexor MVC. Mean ± S.D. values from three subjects on which all measurements were taken are presented, except † values from all six subjects.

Table 2. GL architecture

	Pennation angle (deg)			Fibre length (mm)			Thickness (mm)		
	P	C	D	P	C	D	P	C	D
Rest									
M	10·2 ± 1·2	10·9 ± 1·4	10·2 ± 1·8	72·5 ± 3·6	72·5 ± 2·6	72·5 ± 2·9	15·3 ± 1·2	15·6 ± 0·7	15·5 ± 1·4
MS	11·0 ± 2·0	11·3 ± 1·2†	10·5 ± 1·9	72·0 ± 3·7	74·0 ± 3·4†	73·3 ± 3·8	15·0 ± 1·4	15·2 ± 1·0†	15·5 ± 1·5
L	10·5 ± 2·0	11·0 ± 1·9	11·1 ± 0·6	72·0 ± 3·8	73·0 ± 2·8	72·8 ± 3·0	16·2 ± 2·0	16·0 ± 1·0	15·3 ± 0·6
MVC									
M	35·9 ± 3·2	36·3 ± 2·9	36·4 ± 2·2	33·2 ± 0·6	32·9 ± 3·2	32·2 ± 3·0	22·5 ± 3·0	22·0 ± 3·2	21·8 ± 3·3
MS	37·0 ± 1·5	35·0 ± 2·4†	36·5 ± 0·9	34·0 ± 2·5	35·0 ± 3·0†	34·5 ± 1·5	22·0 ± 2·7	22·0 ± 2·3†	22·0 ± 2·9
L	36·0 ± 2·5	36·9 ± 2·9	36·1 ± 3·0	33·3 ± 3·0	33·8 ± 2·9	33·2 ± 2·5	22·0 ± 0·6	21·0 ± 2·8	21·0 ± 0·8

Analysis of GL architecture at the neutral ankle position along (regions P, C and D) and across (sections M, MS and L) its belly (see Fig. 3), at rest and during an ankle plantarflexor MVC. Mean ± S.D. values from three subjects on which all measurements were taken are presented, except † values from all six subjects.

Table 3. SOL architecture

	Pennation angle (deg)			Fibre length (mm)			Thickness (mm)		
	P	C	D	P	C	D	P	C	D
Rest									
M	25·7 ± 2·6	24·2 ± 2·4	24·9 ± 2·5	36·0 ± 2·8	36·9 ± 2·2	37·2 ± 2·5	14·0 ± 2·0	13·9 ± 2·2	14·2 ± 0·7
MS	25·0 ± 2·2	25·0 ± 2·6†	24·4 ± 2·8	36·8 ± 2·7	35·4 ± 3·5†	36·4 ± 3·5	14·0 ± 2·4	15·1 ± 2·2†	15·0 ± 3·1
L	23·5 ± 2·0	23·8 ± 1·9	22·8 ± 1·7	37·4 ± 2·0	37·0 ± 3·0	37·9 ± 3·0	16·9 ± 1·9	16·0 ± 3·2	15·0 ± 2·5
MVC									
M	39·1 ± 2·5	40·0 ± 0·9	41·3 ± 3·2	32·0 ± 3·8	31·1 ± 2·9	31·5 ± 2·0	20·0 ± 3·0	20·9 ± 2·0	20·1 ± 2·4
MS	40·0 ± 3·4	40·0 ± 3·3†	39·5 ± 2·5	29·5 ± 2·7	30·2 ± 1·9†	30·0 ± 3·0	21·2 ± 2·2	21·0 ± 2·7†	21·8 ± 2·5
L	41·6 ± 3·0	40·4 ± 3·0	39·0 ± 2·1	31·7 ± 3·2	31·7 ± 0·4	32·0 ± 1·9	21·4 ± 3·0	21·8 ± 2·9	22·0 ± 2·2

Analysis of SOL architecture at the neutral ankle position along (regions P, C and D) and across (sections M, MS and L) its belly (see Fig. 3) at rest and during an ankle plantarflexor MVC. Mean ± S.D. values from three subjects on which all measurements were taken are presented, except † values from all six subjects.

0·01) and in SOL from 35 ± 2·6 to 50 ± 2·6 deg (43%, $P < 0·01$). In all three muscles, as ankle angle increased from −15 to +30 deg, fibre length decreased: in GM from 27·2 ± 2·3 to 19 ± 1·8 mm (30%, $P < 0·01$), in GL from 38·2 ± 3·3 to 28 ± 3·1 mm (27%, $P < 0·01$) and in SOL from 35·4 ± 2·1 to 25·6 ± 2·1 mm (28%, $P < 0·01$). Comparing MVC with rest at any given ankle angle, pennation angle was larger and fibre length smaller in all three muscles. In GM, GL and SOL, the pennation angle during MVC was increased by 19–28 deg (90–110%, $P < 0·01$), 23–26 deg (175–256%, $P < 0·01$) and 14–17 deg (50–64%, $P < 0·01$), respectively, and fibre length was reduced by 17–26 mm (47–49%, $P < 0·01$), 27–45 mm (49–54%, $P < 0·01$) and 2–7 mm (7–16%, $P < 0·01$ at −15 deg, $P < 0·05$ at 0 and +15 deg but no significant difference at +30 deg), respectively, compared with rest at any given ankle angle. Thickness of GM at any given ankle angle was not significantly different between rest and MVC. In contrast, thickness of GL and SOL at any given ankle angle increased from rest to MVC by 5–7 mm (36–47%, $P < 0·01$) and 6–7 mm (38–47%, $P < 0·01$), respectively. In GL and SOL the increment was not significantly different either between different imaged sites (regions P, C and D and sections L, MS and M in Fig. 3) at the neutral ankle position or between different ankle positions at a given state of contraction (rest or MVC).

Architectural characteristics during graded isometric force

During graded isometric force up to 100% of MVC at the neutral ankle position, the thickness of GM remained constant (no significant difference) at about 17 mm but the thicknesses of GL and SOL increased gradually from 15 to 22 mm (45%, $P < 0·01$) and from 15 to 21 mm (40%, $P < 0·01$), respectively (Fig. 5*C*). Pennation angle increased and fibre length decreased as a function of contraction intensity in all three muscles. Pennation angle in GM, GL and SOL gradually increased from 22·3 ± 2·0 to 42·5 ± 2·2 deg (95%, $P < 0·01$), from 11·3 ± 1·2 to 38 ± 2·4 deg (245%, $P < 0·01$) and from 25 ± 2·6 to 40 ± 3·3 deg (60%, $P < 0·01$), respectively. Fibre length in GM, GL and SOL decreased gradually from 45 ± 2·3 to 23·4 ± 1·9 mm (49%, $P < 0·01$), from 74 ± 3·4 to 35 ± 3 mm (53%, $P < 0·01$) and from 35·4 ± 3·5 to 30·2 ± 1·9 mm (15%, $P < 0·01$), respectively. Changes in pennation angle as a function of contraction intensity (%MVC) in each muscle were best fitted with a second order polynomial. Regression models are presented in the Appendix.

Comparison between actual and modelled architectural changes

Pennation angles during MVC. Pennation angles during MVC as estimated by the model differed by 0–4 deg (−3 to 10%, $P < 0·01$ at an ankle angle of 0 deg), 9–12 deg (24–38%, $P < 0·01$) and 9–14 deg (25–28%, $P < 0·01$) compared with the corresponding actual pennation angles in GM, GL and SOL, respectively (Fig. 6*A*). The modelled pennation angle at the ankle angle 0 deg in GM was higher than the corresponding actual value but in GL and SOL modelled values were systematically lower than the corresponding actual values.

Pennation angles during graded isometric contraction intensity. Estimated by the model, pennation angles during graded isometric plantarflexion moment differed by 0–4 deg (0–10%, $P < 0·05$ at 60% of MVC and $P < 0·01$ at 80 and 100% of MVC), 2–14 deg (10–36%, $P < 0·05$ at 20% of MVC and $P < 0·01$ at 40, 60, 80 and 100% of MVC) and 3–10 deg (10–26%, $P < 0·01$ at all contraction intensities) from the corresponding actual pennation angles in GM, GL and SOL, respectively (Fig. 6*B*). In GM, modelled pennation angle values were higher than the corresponding actual values at contraction intensities above 60% of MVC but in GL and SOL modelled values were systematically lower than the corresponding actual values.

Fibre lengths during MVC. Fibre length values during MVC as estimated by the model differed by 0–2 mm (0–7%, $P < 0·01$ at an ankle angle of 0 deg), 6–15 mm (22–39%, $P < 0·01$) and 6–8 mm (23–24%, $P < 0·01$) compared with the actual fibre lengths in GM, GL and SOL, respectively (Fig. 6*A*). The modelled fibre length at the ankle angle 0 deg in GM was higher than the corresponding actual value but in GL and SOL modelled values were systematically lower than the corresponding actual values.

Fibre lengths during graded isometric contraction intensity. Estimated by the model, fibre lengths during graded isometric plantarflexion moment differed by 1–2 mm (1–8%, $P < 0·01$ at 40, 60, 80 and 100% of MVC), 5–10 mm (9–28%, $P < 0·01$ at all contraction intensities) and 3–7 mm (9–23%, $P < 0·01$ at all contraction intensities) from the corresponding actual fibre lengths in GM, GL and SOL, respectively (Fig. 6*B*). In GM, modelled fibre length values were systematically higher, and in GL and SOL lower than the corresponding actual values.

Reproducibility of measurements. The central region on the GM mid-sagittal axis was scanned for ten successive days in one subject both at rest and during MVC at the neutral ankle position. In total, thirty measurements were carried out for each architectural characteristic. Care was taken that the same pre-marked area was scanned over the muscle belly in all measurements. The coefficient of variation for the repeat scanning was 2·9% for thickness, 4·3% for fibre length and 4·9% for pennation angle at rest, and 3·9% for thickness, 7·5% for fibre length and 7·8% for pennation angle during MVC. The reproducibility of the digitizing measurements was tested on a GL sonograph that was taken during MVC at the neutral ankle position. Ten measurements were carried out on a given set of architectural characteristics on the same image. The coefficient of variation for repeated measures was 1·2% for thickness, 2·1% for fibre length and 1·6% for pennation angle.

DISCUSSION

The major findings of the present study were that (1) the architecture of the triceps surae complex was homogeneous at the studied sites of the muscle complex, (2) the muscle thickness increased as a function of contraction intensity in GL and SOL but it did not change in GM, and (3) a planimetric model assuming constant thickness and straight fibres did not estimate accurately *in vivo* changes in muscle architecture occurring in the transition from rest to a given isometric contraction intensity.

The similarity in pennation angle, fibre length and thickness values along and across the studied sites over each muscle's belly at a given state of contraction indicated that muscle architecture was consistent over the studied regions and sections in each muscle. As mentioned in Methods, measurements that were taken from the central region over the mid-sagittal axis of each muscle's belly were used as input to the muscle model. It is important to realize that the representativeness of the values that were incorporated in the planimetric model with respect to the architecture of the whole muscle would not affect the validity of the results of our comparisons between actual and modelled muscle architecture, since these were made with respect to a given area of the muscle. Nevertheless, it should be remembered that architectural measurements were taken over a limited area of each muscle and consequently conclusions should not be drawn about the homogeneity in the architecture of the studied muscles over their whole volume. From data concerning the resting length of the human lower limb muscles obtained either from cadavers (Wickiewicz *et al.* 1983; Friendrich & Brand, 1990) or by *in vivo* measurements (Fukunaga *et al.* 1992) and by taking into account the dimensions of the acquired sonographs (9 cm × 3·7 cm), it is estimated that ~47, 51 and 30% of the length of GM, GL and SOL, respectively, was scanned at rest. During

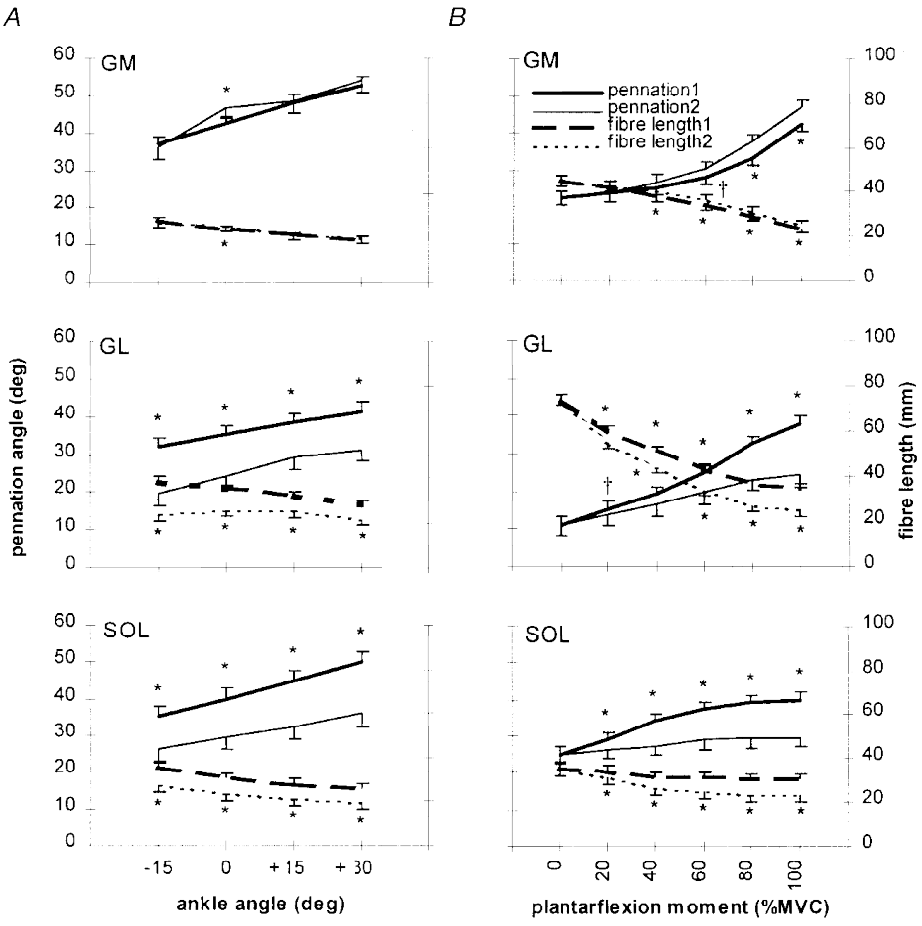

Figure 6. Actual and modelled changes in muscle architecture

Relationships between actual changes (1) and those estimated by a planimetric model (2) in GM, GL and SOL architecture from rest to MVC at each ankle joint angle (*A*) and as a function of contraction intensity at the neutral ankle position (*B*). Values are means ± S.D. ($n = 6$). † and * denote significant difference ($P < 0{\cdot}05$ and $P < 0{\cdot}01$, respectively) between the actual change in an architectural characteristic and that predicted by the model.

isometric plantarflexion Achilles' tendon stretches and since the musculotendon length does not change as force develops, all three muscles shorten, and therefore the relative scanned length over each individual muscle belly during contraction should have been increased compared with the resting state.

In the present study GM pennation angle mean values at the neutral ankle position were larger (by ~5 deg at rest and 7 deg during MVC) and fibre length mean values smaller (by about 5 mm at rest and 10 mm during MVC) than the corresponding values reported by Narici *et al.* (1996). These discrepancies are likely to be due to the difference in the GM length between the two studies; in the present study the knee was flexed at 90 deg, while in that of Narici *et al.* (1996) the knee was fully extended. Since gastrocnemius is a bi-articular muscle crossing both ankle and knee joints, GM and GL would be slacker at any given ankle position at the knee angle of 90 deg than at the knee extension position and this in turn would clearly affect both pennation angle and fibre length. However, an alteration in the knee joint angle at a given ankle angle and state of contraction would not have any effect in SOL architecture since this muscle crosses only the ankle joint.

Differences in the architecture of GM between rest and MVC at any given ankle position were in line with those previously reported by Narici *et al.* (1996). A constancy in GM thickness was visualized whether comparing the resting state with MVC or comparing the different contraction intensities during graded static plantarflexion at the neutral ankle position. However, in both GL and SOL, thickness increased as a function of contraction intensity while in these muscles the model underestimated changes occurring from rest to MVC in both pennation angle and fibre length at any given ankle angle. Therefore, it is reasonable to suggest that changes in GL and SOL thicknesses as a function of contraction intensity may account for the observed differences in these muscles between actual architectural changes and those estimated by the model. A substantial difference between actual and modelled pennation values implies consequences for the validity of calculated individual muscle forces from an analysis incorporating resting pennation values. The force produced by an individual muscle of a group of muscles ending in a common tendon is given by the equation:

$$F_M = (\mathrm{PCSA}/\sum\mathrm{PCSA}) \times F_T/\cos a,$$

where F_M is the force produced in the muscle, PCSA/ΣPCSA is the relative physiological cross-sectional area (rPCSA) of the muscle, F_T is the tendon force and a the pennation angle of the muscle (Narici *et al.* 1992). To quantify the extent of an erroneously calculated F_M during MVC using either cadaveric (Alexander & Vernon, 1975; Wickiewicz *et al.* 1983; Woittiez *et al.* 1983; Friendrich & Brand, 1990; Spoor *et al.* 1991) or modelled MVC pennation data (mean values), we assumed representative values for F_T and rPCSA for each individual muscle and we compared the forces calculated with those derived from incorporating pennation data (mean values) collected in the present study during an ankle plantarflexor MVC. The results presented were derived by incorporating experimentally obtained and modelled pennation data at an ankle angle of −15 deg (the angle at which peak plantarflexor MVC was achieved by all subjects). Incorporation of cadaveric data resulted in an underestimation of ~16, 15 and 10% in forces produced in GM, GL and SOL, respectively, compared with the corresponding calculations derived using experimentally

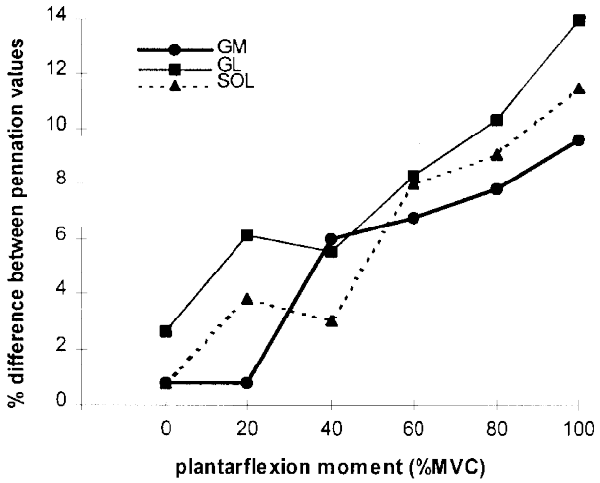

Figure 7. Percentage difference between pennation angle values obtained by digitizing and from the sine formula as a function of contraction intensity at the neutral ankle position

Notice the similarity between the change in fibre curvature (percentage difference between pennation values) as a function of isometric contraction intensity in each muscle in the subjects of the present study ($n = 6$) and the change in intramuscular pressure as a function of isometric contraction intensity in studies by Sejersted *et al.* (1984) and Aratow *et al.* (1993).

observed pennation values during a plantarflexor MVC. An incorporation of modelled pennation values resulted in underestimated forces in GM, GL and SOL by ~1, 10 and 9%, respectively, compared with the corresponding calculations incorporating *in vivo* collected pennation data. Inversely, in an analysis estimating each individual muscle's moment-generating capacity at an ankle angle of −15 deg, use of cadaveric pennation data resulted in overestimated moments by ~20, 17 and 10% in GM, GL and SOL, respectively, compared with the corresponding moments calculated using experimentally collected pennation data. Use of modelled pennation values resulted in overestimated moments in GM, GL and SOL by ~1, 11 and 10%, respectively, compared with the corresponding moments calculated using experimentally collected pennation data. Assuming a ratio between PCSAs in GM : GL : SOL of 2 : 1 : 6 (Wickiewicz *et al.* 1983; Woittiez *et al.* 1983; Friendrich & Brand, 1990; Fukunaga *et al.* 1992), common moment arms (Achilles tendon moment arm), and specific tensions for all three muscles (Woittiez *et al.* 1983), it can be calculated that the above differences would result in an overestimated triceps surae moment-generating capacity of ~14% and 10% using cadaveric and modelled pennation data, respectively, compared with the corresponding moment calculated by incorporating experimentally collected pennation data. At submaximal contraction intensities corresponding to 20, 40, 60 and 80% of MVC at the neutral ankle position, incorporation of cadaveric and modelled pennation data resulted in an overestimation of generated moments of 2–18% (from a moment corresponding to 20% of MVC to a moment corresponding to 80% of MVC) and 4–17% in GL and 1–10% and 3–12% in SOL compared with calculations incorporating the corresponding actual pennation data. In GM, incorporation of cadaveric and modelled pennation data resulted in an overestimation in generated moments at submaximal contraction intensities of 5–20% and in an underestimation of 1–5% (from a moment corresponding to 20% of MVC to a moment corresponding to 80% of MVC) compared with calculations incorporating the corresponding actual pennation data. Triceps surae moments at intensities corresponding to 20, 40, 60 and 80% of MVC were overestimated by ~4, 8, 12 and 16% using cadaveric pennation data and by 2, 5, 6 and 8% using modelled pennation data, compared with moments calculated by incorporating the corresponding experimentally collected pennation data. The above analysis suggests that musculoskeletal models estimating the mechanical output of the triceps surae muscle using either cadaveric (Woittiez *et al.* 1983) or modelled pennation data (Zajac, 1989) may result in unrealistic calculations not only when maximum isometric force is generated, but also in dynamic conditions, when compared with calculations incorporating experimentally collected, force-specific pennation data. Use of the regression model presented in the Appendix would result in an incorporation of force-specific pennation data in all three muscles of the triceps surae complex and a realistic analysis of loads in the lower extremity.

The present study showed that changes in human muscle thickness were not always predictable, but instead appeared to be muscle specific. The thickness of GM did not change in response to contraction intensity but the thicknesses of GL and SOL changed. Our findings concerning a constant thickness in the human GM at different muscle lengths and between different contracting stages are in line with *in vivo* observations of Narici *et al.* (1996) using ultrasonography on the same human muscle. Herbert & Gandevia (1995), using ultrasonography, observed large increases in the human brachialis muscle thickness, when the elbow flexor group produced isometrically a moment equal to 100% of MVC, compared with rest at a given elbow joint angle. Ichinose *et al.* (1995) using ultrasonography found an insignificant but systematic decrease in the resting human vastus lateralis muscle thickness, when a static force equal to 10% of MVC was produced by the knee extensors compared with rest in a series of knee joint angles. However, the decrease became significant when the knee joint was positioned at 80 and 100 deg. Furthermore, Zuurbier & Huijing (1993), by studying *in situ* changes in the rat GM geometry during maximal isometric contractions at different lengths, demonstrated that the assumption of a constant two-dimensional area (derived from the two major assumptions of the model mentioned above), when the muscle is planimetrically modelled as a parallelogram did not hold true. All above observations raise doubts about the applicability of simple planimetric models for describing changes in muscle architecture.

Intramuscular pressure increases as muscle contracts and under isometric conditions there is a positive relationship between contraction intensity and intramuscular pressure (Sejersted *et al.* 1984; Aratow *et al.* 1993). Associated with an increasing intramuscular pressure is an increasing curvature of some of the muscle fibres (e.g. Otten, 1988; Van Leeuwen & Spoor, 1992). When pennation angle from the central mid-sagittal region of each muscle was calculated from the formula $\sin a$ = thickness/fibre length (Kawakami *et al.* 1995), a difference was found compared with the value obtained by digitizing. Pennation values from the sine formula for a given image, set of architectural characteristics and contraction intensity at the neutral ankle position were higher than the respective values derived from digitizing measurements on the superficial aponeurosis of each muscle (angle a in Fig. 2). However, when pennation angles were derived from digitizing measurements on the deep aponeurosis of each muscle (angle b in Fig. 2), the sine formula gave lower pennation values. For a given muscle, the absolute value of the difference between pennation values obtained by digitizing and with the sine formula was of a similar level between aponeuroses. The difference between pennation values obtained from the two different approaches indicated a curving fibre shape in each muscle. The similarity between the latter percentage difference between the pennation values–contraction intensity curve (Fig. 7) and the intramuscular pressure–contraction

intensity curve (Sejersted *et al.* 1984; Aratow *et al.* 1993) supports in an indirect but correlational way an association between intramuscular pressure and fibre curvature. The similarity of the absolute value of the above difference between the superficial and deep aponeuroses of the same muscle indicated a homogeneous curvature at the respective insertion points, implying no alteration in the loss of force transmitted to the tendon during contraction calculated according to the sine formula. When a muscle is planimetrically represented as a parallelogram the fibres are modelled as straight lines between aponeuroses. The measurement of fibre length along a straight line in the present study was to enable the application of such a model. The morphometric analysis performed indicated, however, that fascicles curved as a function of contraction intensity. Changes in fibre curvature are not taken into account when using simple planimetric models. However, more complex muscle models allow incorporation of the curving fibre shape and aponeuroses orientation during muscle contraction (Van Leeuwen & Spoor, 1992).

As intramuscular pressure builds up during contraction, the muscle becomes less compliant in the direction of its thickness. The line of action of the effective muscle fibre force transmitted to the tendon lies on the longitudinal axis of the tendon. The point at which the muscle's distal tendon is attached remains constant during contraction. However, the spatial orientation of the longitudinal axis of the tendon may change when contraction results in an increased muscle thickness in a muscle adjoining bones and other rigid tissue, such as in co-activated synergist, stabilizer and antagonist muscles. Thus, an increased muscle thickness as a result of a high contraction intensity may have implications for the magnitude of the musculotendon moment arm involved and calculation of the respective developed moment. In the case of GM, GL and SOL whose distal tendons join to form the Achilles tendon, a high contraction isometric plantarflexion may result in a displacement of the Achilles tendon relative to its resting position due to an increased thickness in GL and SOL during contraction compared with rest.

In conclusion, this study showed that both pennation angle and fibre length of all three muscles of the triceps surae complex are consistent over a major part of the muscle and change both in response to changes in ankle angle at rest and during isometric contractions at intensities up to 100% of plantarflexor MVC. Changes in individual muscle architecture in transition from rest to a given contraction intensity were not always predictable by a model representing the muscle planimetrically as a parallelogram. Changes in a muscle's pennation angle should be taken into account and modelled accordingly when either individual muscle forces or generated moments are to be estimated.

APPENDIX

Regression models describing changes in pennation angle (a) in GM, GL and SOL as a function of isometric plantarflexion moment (% MVC) in the present study are:

GM: $a = 0{\cdot}002443 \times (\%\mathrm{MVC})^2 - 0{\cdot}05286 \times (\%\mathrm{MVC}) + 22{\cdot}90574$ ($r^2 = 0{\cdot}99$, $P < 0{\cdot}001$).

GL: $a = 0{\cdot}000906 \times (\%\mathrm{MVC})^2 + 0{\cdot}182805 \times (\%\mathrm{MVC}) + 11{\cdot}2036$ ($r^2 = 0{\cdot}99$, $P < 0{\cdot}001$).

SOL: $a = -0{\cdot}00131 \times (\%\mathrm{MVC})^2 + 0{\cdot}287395 \times (\%\mathrm{MVC}) + 24{\cdot}5929$ ($r^2 = 0{\cdot}99$, $P < 0{\cdot}001$).

Alexander, R. McN. & Vernon, A. (1975). The dimensions of knee and ankle muscles and the forces they exert. *Journal of Human Movement Studies* **1**, 115–123.

Aratow, M., Ballard, R. E., Crenshaw, A. G., Styf, J., Watenpaugh, D. E., Kahan, N. J. & Hargens, A. R. (1993). Intramuscular pressure and electromyography as indexes of force during isokinetic exercise. *Journal of Applied Physiology* **74**, 2634–2640.

Baskin, R. J. & Paolini, P. J. (1967). Volume change and pressure development in muscle during contraction. *American Journal of Physiology* **213**, 1025–1030.

Friendrich, J. A. & Brand, R. A. (1990). Muscle fibre architecture in the human lower limb. *Journal of Biomechanics* **23**, 91–95.

Fukunaga, T., Kawakami, Y., Kuno, S., Funato, K. & Fukashiro, S. (1997). Muscle architecture and function in humans. *Journal of Biomechanics* **30**, 457–463.

Fukunaga, T., Roy, R. R., Shellock, F. G., Hodgson, J. A., Day, M. K., Lee, P. L., Kwong-Fu, H. & Edgerton, V. R. (1992). Physiological cross-sectional area of human leg muscles based on magnetic resonance imaging. *Journal of Orthopaedic Research* **10**, 926–934.

Gans, C. (1982). Fibre architecture and muscle function. *Exercise and Sport Sciences Reviews* **10**, 160–207.

Gans, C. & Bock, W. J. (1965). The functional significance of muscle architecture: a theoretical analysis. *Ergebnisse der Anatomie und Entwicklungsgeschichte* **38**, 115–142.

Henriksson-Larsen, K., Wretling, M.-L., Lorentzon, R. & Oberg, L. (1992). Do muscle fibre size and fibre angulation correlate in pennate human muscles? *Pflügers Archiv* **64**, 68–72.

Herbert, R. T. & Gandevia, S. C. (1995). Changes in pennation with joint angle and muscle torque: *in vivo* measurements in human brachialis muscle. *Journal of Physiology* **482**, 523–532.

Huijing, P. A. & Woittiez, R. D. (1984). The effect of architecture on skeletal muscle performance: A simple planimetric model. *Netherlands Journal of Zoology* **34**, 21–32.

Ichinose, Y., Kawakami, Y. & Fukunaga, T. (1995). In vivo measurement of fascicle arrangement in human vastus lateralis muscle using ultrasound. In *XVth Congress of the International Society of Biomechanics*, ed. Hakkinen, K., Keskinen, K. L., Komi, P. V. & Mero, A., pp. 412–413. Gummerus, Jyvaskyla, Finland.

Kawakami, Y., Abe, T. & Fukunaga, T. (1993). Muscle-fibre pennation angles are greater in hypertrophied than in normal muscles. *Journal of Applied Physiology* **74**, 2740–2744.

Kawakami, Y., Abe, T., Kuno, S.-Y. & Fukunaga, T. (1995). Training-induced changes in muscle architecture and specific tension. *European Journal of Applied Physiology* **72**, 37–43.

Kawakami, Y., Nakazawa, K., Fujimoto, T., Nozaki, D., Miyashita, M. & Fukunaga, T. (1994). Specific tension of elbow flexor and extensor muscles based on magnetic resonance imaging. *European Journal of Applied Physiology* **68**, 139–147.

Muhl, Z. F. (1982). Active length-tension relation and the effect of muscle pennation on fibre lengthening. *Journal of Morphology* **173**, 285–292.

Narici, M. V., Binzoni, T., Hiltbrand, E., Fasel, J., Terrier, F. & Cerretelli, P. (1996). *In vivo* human gastrocnemius architecture with changing joint angle at rest and during graded isometric contraction. *Journal of Physiology* **496**, 287–297.

Narici, M. V., Capodaglio, P., Minetti, A. E., Ferrari-Bardile, A., Maini, M. & Cerretelli, P. (1998). Changes in human skeletal architecture induced by disuse-atrophy. *Journal of Physiology* **506.P**, 59–60*P*.

Narici, M. V., Landoni, L. & Minetti, A. E. (1992). Assessment of human knee extensor muscles stress from *in vivo* physiological cross-sectional area and strength measurements. *European Journal of Applied Physiology* **65**, 438–444.

Otten, E. (1988). Concepts and models of functional architecture in skeletal muscle. *Exercise and Sports Science Reviews* **16**, 89–137.

Rutherford, O. M. & Jones, D. A. (1992). Measurement of fibre pennation using ultrasound in the human quadriceps *in vivo*. *European Journal of Applied Physiology* **65**, 433–437.

Sejersted, O. M., Hargens, A. R., Kardel, K. R., Blom, P., Jensen, O. & Hermansen, L. (1984). Intramuscular fluid pressure during isometric contraction of human skeletal muscle. *Journal of Applied Physiology* **56**, 287–295.

Spoor, C.W., Van Leeuwen, J. L., Van der Meulen, W. J. T. M. & Huston, A. (1991). Active force-length relationship of human lower-leg muscles estimated from morphological data: a comparison of geometric muscle models. *European Journal of Morphology* **29**, 137–160.

Van Leeuwen, J. L. & Spoor, C. W. (1992). Modelling mechanically stable muscle architectures. *Philosophical Transactions of the Royal Society* B **336**, 275–292.

Wickiewicz, T. L., Roy, R. R., Powel, P. L. & Edgerton, V. R. (1983). Muscle architecture of the human lower limb. *Clinical Orthopaedics and Related Research* **179**, 275–283.

Woittiez, R. D., Huijing, P. A., Boom, H. B. K. & Rozendal, R. H. (1984). A three-dimensional muscle model: a quantified relation between form and function of skeletal muscle. *Journal of Morphology* **182**, 95–113.

Woittiez, R. D., Rozental, R. H. & Huijing, P. A. (1983). The functional significance of architecture of the human triceps surae muscle. In *Biomechanics IX-A*, ed. Winter, D. A., Norman, R. W., Wells, R. P., Hayes, K. C. & Patla, A. E., pp. 21–26. Human Kinetics Publishers, Inc., Champaign, IL, USA.

Yamaguchi, G. T., Sawa, A. G. U., Moran, D. W., Fessler, M. J. & Winters, J. M. (1990). A survey of human musculotendon actuator parameters. In *Multiple Muscle Systems: Biomechanics and Movement Organization*, ed. Winters, J. M. & Woo, S. L.-Y., pp. 713–773. Springer-Verlag, New York.

Zajac, E. F. (1989). Muscle and tendon: Properties, models, scaling, and application to biomechanics and motor control. *Critical Reviews in Biomedical Engineering* **17**, 359–411.

Zuurbier, C. J. & Huijing, P. A. (1993). Changes in geometry of actively shortening unipennate rat gastrocnemius muscle. *Journal of Morphology* **218**, 167–180.

Corresponding author

C. N. Maganaris: Biomechanics and Neuromuscular Biology Research Groups, Manchester Metropolitan University, Alsager ST7 2HL, UK.

Email: c.maganaris@mmu.ac.uk